SOYBEAN RESPONSE TO INITIAL STAGE OF *Fusarium virguliforme* INFECTION

María Lorena Giachero[1-2], Nathalie Marquez[1-2], Leandro Ismael Ortega[1], Daniel Adrian Ducasse[1-2†]

1. Instituto Nacional de Tecnología Agropecuaria, Centro de Investigaciones Agropecuarias (INTA-CIAP)

2. Instituto de Patología Vegetal (IPAVE), Av. 11 de Septiembre 4755, X5014MGO, Córdoba, Argentina.

3. Consejo Nacional de Investigaciones Científicas y Técnicas, Unidad de Fitopatología y Modelización Agrícola (CONICET-UFyMA), Av. 11 de Septiembre 4755, X5014MGO, Córdoba, Argentina.

† Deceased 11 May, 2020

The e-mail address of the corresponding author: giachero.lorena@inta.gob.ar

KEYWORDS: Sudden Death Syndrome; lignin; suberin; cell wall

ABSTRACT

Fusarium virguliforme causes the Sudden Death Syndrome, an important disease in soybean crops. In this work, we investigated the defensive response mechanisms in soybean root, at cell wall level, during *F. virguliforme* infection using an in vitro culture system. We measured total root lignin content by the acetyl bromide method and estimated the in-situ lignin and suberin deposition by confocal microscopy on local and systemic root tissues, i.e. adjacent and distant to the pathogen entry site respectively. Moreover, the expression dynamics of phenylalanine ammonia lyase (PAL), shikimate/quinate hydroxycinnamoyltransferase

(HCT) and cinnamyl alcohol dehydrogenase (CAD) was evaluated by real-time quantitative PCR. The results showed that, although the most significant increment of lignin deposition was observed in the epidermal cells of local tissues, *F. virguliforme* also induced lignin deposition changes in a sistemic fashion. In fact, inoculated plants presented a higher deposition of lignin in hypodermis and cortex than the control ones, independently of the distance from the inoculum source, while suberin deposition was higher in local zones. Moreover, the gene expression analysis showed an up-regulation of PAL, HCT and CAD genes after the inoculation with the pathogen, which correlates with the cell wall modifications observed in the local tissues. The results presented here suggest that the increase in lignin and suberin deposition during soybean root/*F. virguliforme* interaction is probably a strategy not only to stop the pathogen entrance, but to provide the plant more time to prepare its defences as well.

1. INTRODUCTION

In 2020, the world soybean production reached around 350 million tons over 126.9 million ha. Climate, land extension, and soil conditions turn Brazil (121.8 million tn), United States (112.5 million tn) and Argentina (48.8 million tn) the major world soybean producers (FAOstat 2021). On the other hand, these geographical regions may have optimal conditions for the occurrence of soybean diseases and consequently yield losses (Wrather et al. 2010). Sudden Death Syndrome (SDS) is one of these diseases and it is ranked as the most destructive for this crop worldwide (Wrather et al. 2010). SDS is caused by a complex of at least four species of *Fusarium* sp.: *F. virguliforme, F. tucumaniae, F. brasiliense* and *F. crassistipitatum* (Aoki et al. 2005, 2012). However, *F. virguliforme* is the most geographically distributed (Spampinato et al. 2021). The colonization of these fungi is

generally restricted to roots, however SDS causes both root and leaf symptoms. Root symptoms include crown rotting and vascular tissue discoloration, while leaf symptoms consist in typical chlorotic interveinal spots that can coalesce and eventually become necrotic (Roy 1997; Rupe et al. 2001). The toxins produced by the pathogen in roots are responsible for foliar symptoms (Brar et al. 2011; Abeysekara and Bhattacharyya 2014). The severity of foliar symptoms of SDS is associated with soil temperature (22 to 24°C) and soybean age, given plants are more susceptible to infection at early stages of development (Gongora-Canul et al. 2011).

F. virguliforme is a hemi-biotrophic pathogen (Roy et al. 1997), initially behaving as a biotrophic and later switching to a necrotrophic phase (Iqbal et al. 2005). Navi et al. (2008) showed that *F. virguliforme* forms appressoria and infection pegs to penetrate the host root. In a comparative transcriptome analysis of *F. virguliforme* infection process, Sahu et al. (2017) found an upregulation of genes related to the degradation of antimicrobial compounds such as phytoalexin and glycoline during the early stages of root tissue infection. Meanwhile, in late infection stages, many genes encoding hydrolytic and catalytic enzymes were up-regulated (Sahu et al. 2017). An important component of pathogen attack are the cell wall degrading enzymes (CWDEs). A recent study has shown that also it is likely that *F. virguliforme* employs CWDE as pathogenicity factors (Islam et al., 2017). Plants can prevent pathogen infection by inactivating CWDEs, through secreting inhibitor proteins (PIPs) (Chang et al. 2016; Misas-Villamil and Van der Hoorn 2008). Interestingly, two xylanases of *F. virguliforme* related to cell wall degradation, were detected as potential targets for exogenous PIPs (Chang et al. 2016).

Several studies have been carried out to characterize the plant response to *F. virguliforme* colonization. During soybean infection, genes related to defense, signal recognition and

transduction, cell wall synthesis and metabolic processes were differentially expressed (Iqbal et al., 2005; Nagki et al., 2016; Marquez et al., 2019; Radwan et al., 2011). A large number of these up-regulated genes encode cell wall and plasma membrane related proteins (Ngaki et al., 2016). Curiously, even though phenylpropanoid biosynthesis was the metabolic pathway with the highest number of differentially expressed genes, Marquez et al. (2019) observed the downregulation of a considerable number of cell wall and signalling-related genes in presence of *F. virguliforme*. Similarly, previous soybean transcriptome studies showed an induction of the phenylpropanoid pathway after inoculation with *Fusarium solani* f. sp. *Glycines* (Lozovaya et al., 2004; Iqbal et al., 2005). Apparently, the soybean roots of partially resistant genotypes display high rate of lignification immediately post infection (Lozovaya et al. 2006). This result shows that lignin is playing a key role in the defence against this pathogen. Moreover, Iqbal et al. (2005) suggest that, in addition to the phenylpropanoid pathway, the partially resistant soybean genotypes to SDS are capable of recognizing the pathogen through receptors similar to kinases (RLK) as an early defence mechanism.

The structure and composition of plant cell wall is dynamic, and can be remodeled during development or in response to the environment (Liu et al. 2018). The cell wall, in addition to being a physical barrier against pathogen invasion, has been proposed as a monitor system. Plants can detect modifications in the cell wall and trigger immune responses, through protein kinases and calcium signaling (Wolf 2017). Lignin is one of the main and most widespread cell wall strengtheners in the Tracheophyta (Zhong et al. 2011). Lignin biosynthesis is often induced at the site of pathogen attack providing a physical barrier against infection (Bonello et al. 2003; Buendgen et al. 1990). Likewise, suberin also constitutes a pathogen-induced defence response. Suberization occurs in specific sites of the roots (Thomas et al. 2007)

97 forming a physical barrier and preventing water loss through exposed and injured tissues
98 (Kolattukudy 2001; Franke and Schreiber 2007).
99 The main purpose of this work was to investigate, at cell wall level, the defensive response
100 mechanisms in soybean root during the early steps of *F. virguliforme* infection using an in
101 vitro culture system. Therefore, the present study aims were 1) to quantify total root lignin
102 content, 2) to observe the pattern of in-situ lignin and suberin deposition and distribution in
103 two roots sampling zones: local (adjacent to the pathogen entry - FvA) and systemic (distant
104 to the pathogen entry - FvD) and 3) to evaluate the expression levels of lignin-related
105 biosynthetic pathway genes (local and systemic).
106

107 ## 2. MATERIALS AND METHODS

108 ### 2.1 Biological Material

109 *F. virguliforme* (Syn. *F. solani* f. sp. *glycines*) (*Fusarium virguliforme* O'Donnell & T. Aoki)
110 obtained from soybean (*Glycine max*) in Argentina (Buenos Aires, San Pedro) (Aoki et al.
111 2005) was grown on Potato Dextrose Agar (PDA) (Scharlau Chemie S.A, Barcelona, Spain)
112 at 25°C in the dark for seven days.
113 Soybean seeds [*Glycine max* (L.) Merr.] cv SPS 4x4RR (Syngenta□) were surface-
114 disinfected following protocol descript by Giachero et al. (2017). After disinfection, groups
115 of 6 seeds were germinated per Petri dish (Ø145 mm) with 1% (w/v) water-agar
116 supplemented with 0.8% sucrose. The Petri dishes were kept in the dark at 25°C for 4 days,
117 and then exposed to light for 24 h (average photosynthetic photon flux of 225 μmol m−2
118 s−1).
119

120 ### 2.2 Experimental design

Soybean plantlets (5 days old) were transferred to an *in vitro* system containing Modified Strullu-Romand (MSR) medium (Declerck et al. 1998) without sucrose and vitamins, and solidified with 3 g l^{-1} Phytagel (Sigma-Aldrich, St. Louis, USA). Plantlets roots were placed on the surface of the medium and the shoots were let extrude the Petri dish through a hole in the lid (Giachero et al. 2017). These *in vitro* systems were incubated in a growth chamber at 25ºC, 70% of relative humidity, and 16 h/day photoperiod with a 300 µmol$m^{-2}s^{-1}$ photosynthetic photon flux. The dishes were covered to avoid light incidence on the roots. After fifteen days, the *in vitro* systems were randomly divided into two groups corresponding with two treatments: one control without *F. virguliforme* inoculation (C) and the other one, inoculated with *F. virguliforme* (Fv). The inoculation protocol was performed as described by Giachero et al (2017) using a 7 days old plug from a *F. virguliforme* culture in PDA. Root samples were taken from both treatments at 24, 48, 72 and 96 hours post-inoculation (hpi) for the determinations described in the next sections.

2.3 Root lignin content determination by Acetyl bromide method

This method allows an in-bulk determination of the lignin content of whole plant organs. To determine lignin content in soybean roots, the acetyl bromide protocol descript by Moreira-Vilar et al. (2014) was used with modifications.

The absorbance of the samples was measured at 280 nm. A standard curve was generated using Kraft lignin (Sigma-Aldrich®) and the results were expressed as lignin (mg) per cell wall (g). Four biological replicates were considered for each treatment at every time point.

2.4 *In-situ* lignin and suberin estimation by confocal microscopy

144 *In-situ* lignin and suberin deposition was estimated as described by Hutzler et al. (1998)
145 taking advantage of the auto-fluorescent properties of these biopolymers (Vaughn and Lulai
146 1991).
147 Root segments of 2 cm in length, were sampled from a site near to the pathogen entry (FvA,
148 local) and distant from that point (FvD, systemic) (Figure 1a). The segments corresponded
149 to the root maturation zone (Figure 1b), i.e. 1 cm from the root apex. Transverse free-hand
150 sections were performed at 5mm intervals along the fragment, which were immediately fixed
151 in FAA (formaldehyde, acetic acid, EtOH, 2:1:17) for half an hour and mounted onto glass-
152 slides with a drop of 50% glycerol. Observations were done in a Nikon Eclipse CS1 spectral
153 confocal microscope, using a 400 nm diode laser at 10% power as light source. In preliminary
154 experiments, the emission was analysed with the spectral detector (28 channels, 10 nm
155 resolution) in the different zones to be examined: epidermis (e), hypodermis (h), cortex (c)
156 and endodermis (en, Figure 1c). Differential spectra attributed to lignin and suberin were
157 successfully discriminated (data not shown). From these results, the correspondence between
158 emission peaks of each biopolymer and the emission filters range of the conventional
159 confocal mode detectors was observed. Thus, this acquisition mode was used henceforth for
160 the rest of the analyses. Auto-fluorescence emission, due to lignin and suberin, was imaged
161 through BP450/35 (“blue” channel) and BP605/75 (“red” channel) emission filters,
162 respectively. Images were acquired setting 10 µs of laser dwell-time and a 1024x1024 dpi
163 resolution. Average pixel gray value in each channel was measured inside delimited areas,
164 using the open source software FIJI (Schindelin et al. 2012). Four biological replicates per
165 treatment in each time point of sampling, were used in each case. This experiment was
166 performed twice.

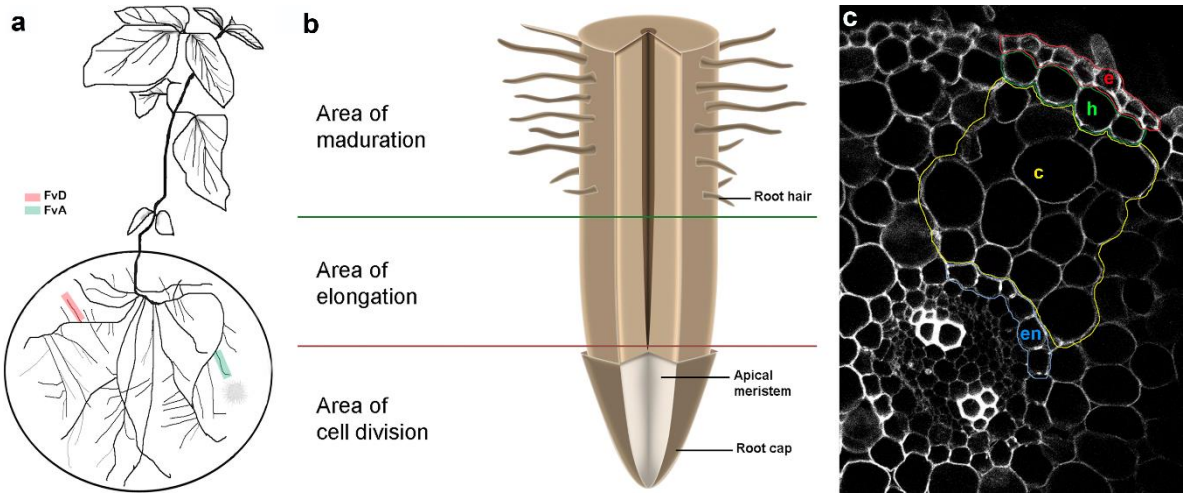

Figure 1 (**a**) Schematic representation of the in vitro culture system used to grow soybean plants in Petri dishes with Phytagel medium. The figure shows the two sampling sites of the root system, adjacent (FvA) and distant (FvD) to the pathogen inoculation point. (**b**) Schematic view (not at scale) of the different zones of the root tip. Segments from the maturation zone were sampled for sectioning and observation. (**c**) Representative image showing the four evaluated areas: epidermis (e), hypodermis (h), cortex (c) and endodermis (en).

2.5 Gene expression analysis by real-time quantitative RT-PCR

Root segments of 2 cm in length were sampled from C (control), FvA (local) and FvD (systemic) at 24, 48, and 72 hpi with *F. virguliforme*.

Total RNA was extracted using the Trizol® reagent (Invitrogen, Carsbad, USA) according to manufacturer's instructions with an additional chloroform purification step. All samples were treated with DNAse I Amplification Grade (Invitrogen Life Technologies) according to the manufacturer's instructions. Concentration and purity of total RNA were determined (A260/280 absorbance ratio) using a NanoDrop®-ND 1000 UV-Vis Spectrophotometer (NanoDrop Technologies, Wilmington, USA).

Real-time quantitative RT-PCR (qPCR) was performed using the Rotor Gene 6000 with the iTaqTM Universal SYBR® Green Supermix (BIORAD, catalog 172-5151) and specific primers for the following genes: Phenylalanine ammonia lyase 1 (PAL 1), Cinnamyl alcohol dehydrogenase (CAD), Shikimate O-hydroxycinnamoyltransferase (HCT) (Supplementary table 1). The thermal cycling protocol was: 50ºC for 10 min, 95ºC for 1 min, amplification and quantification cycles repeated 40 times 95ºC for 15 s, 61ºC for 30 s, followed by melting curve data collection to check for non-specific amplification and primer dimers. Three independent biological replicates, each consisting of a pool of two soybean root samples, with two technical replicates were analyzed per treatment. Normalization was achieved using the SKIP16 reference gene (Hu et al. 2009), which showed to be stable under the tested conditions. Relative gene expression was calculated using the $2^{-\Delta\Delta Ct}$ method (Livak and Schmittgen, 2001). The amount of target transcripts in control roots (C) was considered as basal level during expression analysis.

2.6 Assessment of colonization by *F. virguliforme*

The root samples for assessment of infection by *F. virguliforme* were taken at the end of assay (i.e. 96 hpi). Colonization by *F. virguliforme* was followed under the microscope (Nikon labophot-2, Japan) at 10–40× magnification. Roots were cleared in 10% KOH at room temperature for 3 h, rinsed with distilled water, bleached and acidified with HCl 1% and stained with Trypan blue 0.2% at room temperature overnight.

2.7 Statistical analysis

Data were subjected to analysis of variance (ANOVA) ($p \leq 0,05$ level of significance). The LSD Fisher post-hoc test was used to discriminate differences in lignin and suberin content

209 results (spectrophotometry and microscopy) and the DGC test for the qPCR experiments. An
210 α=0.05 was used in all cases. All the analyses were performed using the INFOSTAT software
211 (Di Rienzo et al. 2008).
212
213 **3. RESULTS**
214 **3.1 Lignin and suberin content**
215 Lignin content in the total root system, determined by the acetyl bromide method, did not
216 show significant differences between treatments during the evaluated time points (Figure 2).
217 Since this approach could overlook differences in lignin deposition at cell wall level, the root
218 maturation zone was examined by cross-sections (Figure 3). This analysis showed that the
219 amount of lignin was different between treatments. Using a semi-quantitative estimation by
220 Average Grey Value (AGV) of microscopy images, we observed that *F. virguliforme*
221 inoculation induced changes in lignin deposition. Both FvA and FvD zones showed a
222 significant increase in lignin content with respect to non-inoculated root (C) at 48 and 96 hpi
223 with an apparent higher increase in FvD at 48 hpi (Figure 3a,c). Irrespective to time, the root
224 epidermis (e) showed the highest AGV in all treatments with a significant increase in the
225 adjacent zone of the inoculated plants (Figure 3b). Both hypodermis (h) and cortex (c) of
226 inoculated plants, from either FvA and FvD segments, showed higher AGVs with respect to
227 controls (Figure 3b). No differences were detected in the endodermis (data not shown).
228 Suberin was detected both in epidermis and hypodermis cells exhibiting auto-fluorescence in
229 tangential and radial cell walls. This auto-fluorescence was higher in epidermal than
230 hypodermal cells (Figure 4b). AGVs were significantly higher in FvA zones only at 24 hpi
231 (Figure 4a,c). The figure 4c shows a detailed image of both epidermis and hypodermis, where
232 a high difference in the auto-fluorescence emission due to suberin ("red" channel) in FvA

233 zones 24 hpi, was observed. As with lignin, no differences were detected in the endodermis
234 (data not shown).
235

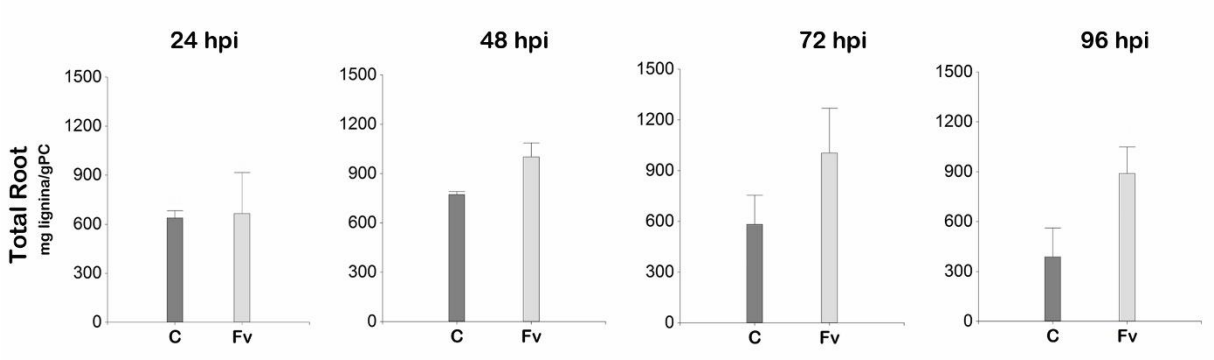

236

237 **Figure 2** Lignin content of soybean root determined by the acetyl bromide method. C:
238 control, Fv: roots of soybean inoculated with *F. virguliforme*. The results were expressed as
239 mg lignin g-1 cell wall. Mean values ± SE (n = 3) marked with different letters are
240 significantly different ($p \leq 0,05$ ANOVA and LSD Fisher α=0,05)
241

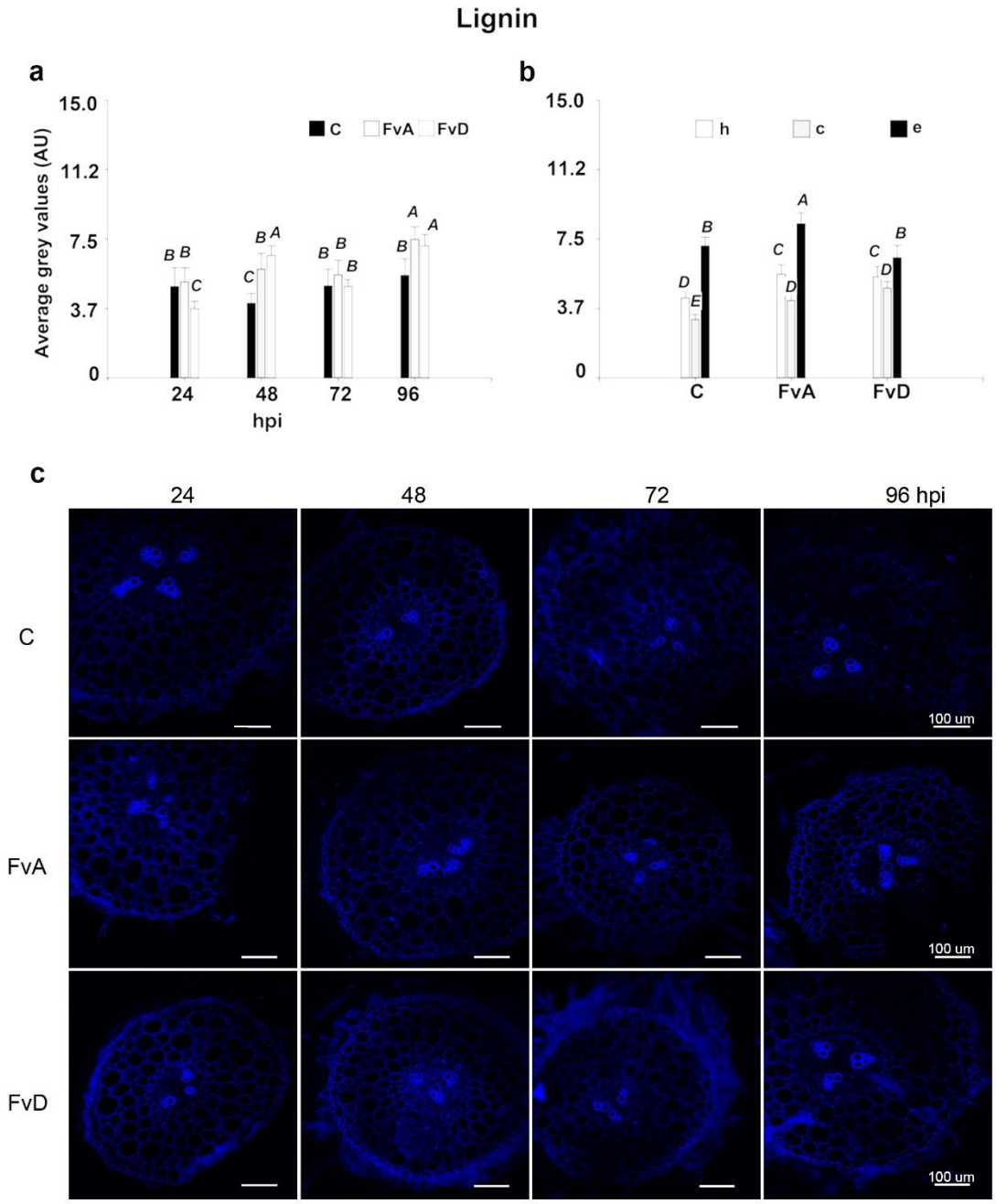

Figure 3 Lignin deposition in soybean roots (**a** and **b**) expressed like average grey values (AU: Arbitrary Units). FvA: adjacent to the Fv inoculation; FvD: distant area to the pathogen inoculation point; C: control; hpi: hours post inoculation. Evaluated areas: epidermis (e), hypodermis (h), cortex (c). Mean values ± SE (n = 3) marked with different letters are significantly different ($p \leq 0,05$ ANOVA and LSD Fisher $\alpha=0,05$). Imaging of transverse free-hand sections in soybean roots (**c**). Observations were done in a Nikon Eclipse CS1 spectral

confocal microscope. Auto-fluorescence emission due to lignin was imaged through BP450/35 ("blue" channel) emission filters.

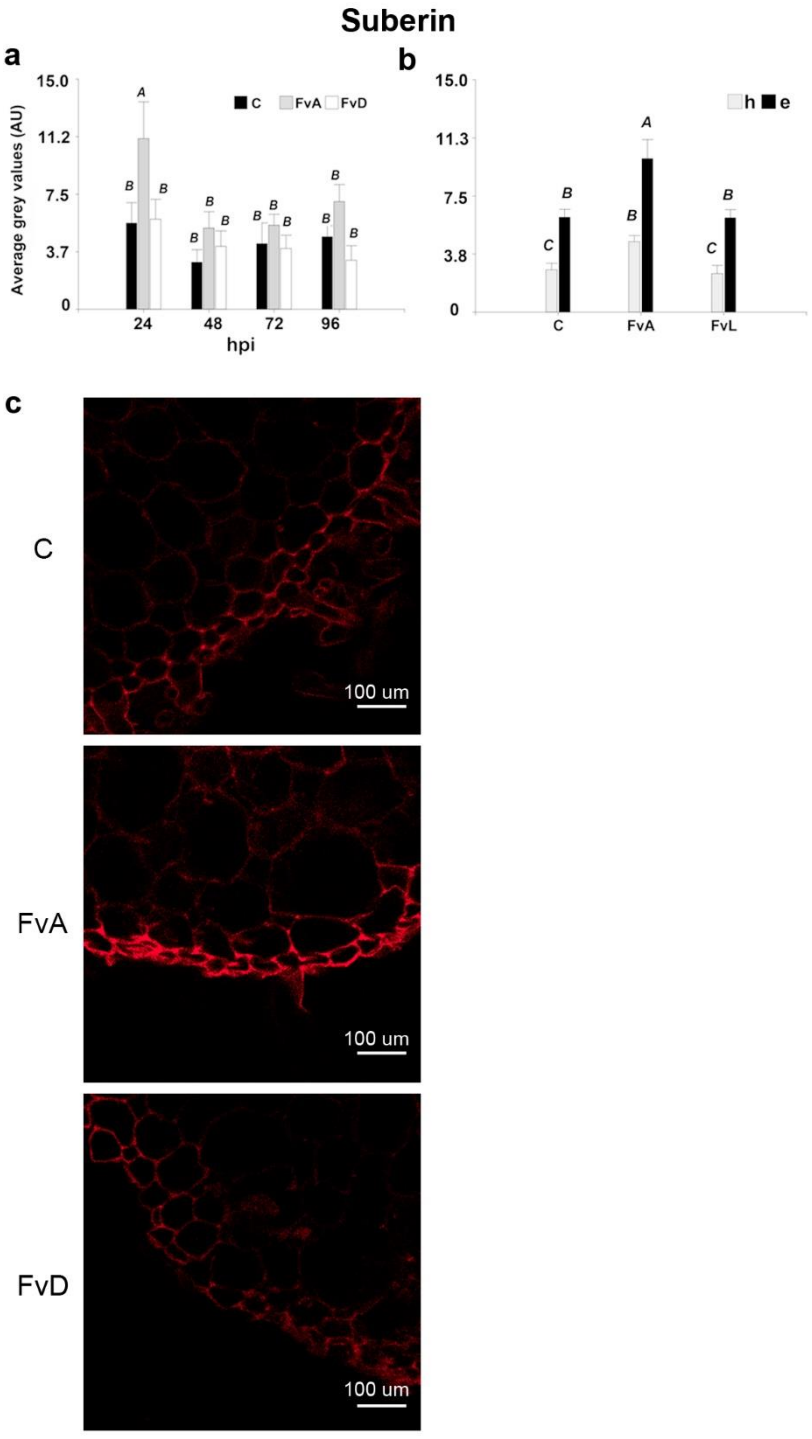

Figure 4 Suberin deposition in soybean roots (**a** and **b**) expressed like average grey values (AU: Arbitrary Units). FvA: adjacent to the Fv inoculation; FvD: distant area to the pathogen

inoculation point; C: control; hpi: hours post inoculation. Evaluated areas: epidermis (e), hypodermis (h), cortex (c). Mean values ± SE (n = 3) marked with different letters are significantly different ($p \leq 0,05$ ANOVA and LSD Fisher $\alpha=0,05$). In b, interaction between treatments and sampling zones was not significant ($p \leq 0,05$). Nevertheless, comparisons of all the means involved in the interaction were assessed. Detailed image of epidermis and hypodermis in transverse free-hand sections in soybean roots (**c**) shows a difference in Auto-fluorescence emission due to suberin at 24 hpi. The image was imaged through BP605/75 ("red" channel) emission filters.

3.2 Gene expression analysis

The expression dynamics of three genes (PAL, HCT and CAD) was evaluated by real-time quantitative PCR in both treatments: inoculated with *F. virguliforme* (Fv) and non-inoculated (C) soybean roots at 24, 48, and 72 hpi. Two sampling areas were evaluated in the root system: adjacent (FvA) and distant (FvD) to the pathogen inoculation point.

Interaction between treatments, time (hpi) and sampling zones, was not significant ($p \leq 0,05$) for the analysed genes. Nevertheless, comparison of all the means involved in the interaction was assessed.

The results (Figure 5) showed that PAL 1, HCT and CAD genes were significantly induced by *F. virguliforme*. However, the expression levels were similar among the three post-inoculation times analysed. Moreover, when soybean root sampling areas were compared, results showed that transcriptional changes of PAL 1, HCT and CAD genes were significantly higher in the adjacent area (FvA) than the distant area (FvD) to the pathogen inoculation point.

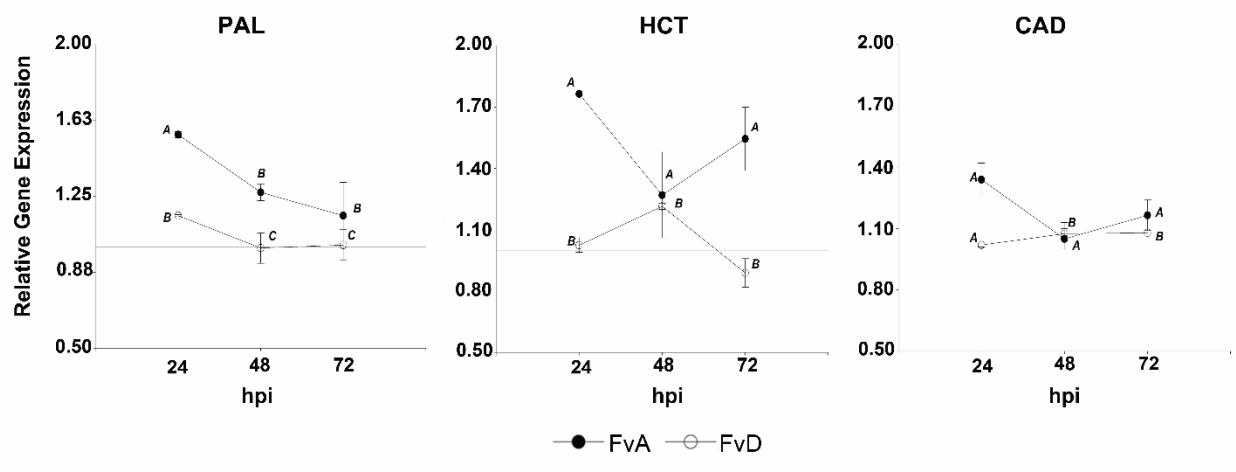

Figure 5 Quantitative RT-PCR of genes involved in the lignin biosynthesis pathway (PAL, HCT and CAD) in 2-week-old soybean roots in response to *Fusarium virguliforme* inoculation. Two sampling areas were evaluated in the root system: adjacent (FvA: dark spot) and distant (FvD: clear spot) to the pathogen inoculation point at 24, 48, and 72 hpi with *F. virguliforme*. Data are means of three biological replicates (n=3). The mean values and standard errors were calculated from two technical replicates. Transcript levels are expressed relative to non-inoculated soybean plantlets (C). Different letters indicate significant differences (DGC Alfa=0,05)

3.3 *F. virguliforme* colonization

The hyphae of *F. virguliforme* reached the soybean root surface at 48 h after inoculation. Following this first contact, hyphae development within the root could not be confirmed by microscopic observation and soybean roots did not show any disease symptoms.

4. DISCUSSION

In the current study, using an in vitro culture system, cell wall modification in soybean root composition was analysed during the early steps of *F. virguliforme* infection. Previous studies reported that different types of biotic stresses can raise lignin and suberin deposition in cell walls to block pathogen invasion and to reduce the host susceptibility (Moura et al.

2010; Thomas et al. 2007). Therefore, in a first assay, the amount of lignin was evaluated in the total root. Results showed a trend of increased lignin deposition in inoculated plants by the time course. However, this correlation could not be confirmed statistically when the roots were evaluated as a whole organ. Lignin deposition is a tissue specific process, occurring in key plant development processes as the conductive tissue maturation, which is fundamental for the proper function of xylem vessels (Barros et al. 2015). Moreover, several reports, have suggested that lignin biosynthesis is induced at the site of pathogen infection providing a physical barrier (Bonello et al. 2003; Buendgen et al. 1990) which may limit further growth and / or confine invading pathogens (Menden et al. 2007; Smit and Dubery, 1997; Wuyts et al. 2006). Thus, it is possible that this localized lignin deposition, induced by the defence response, be diluted in the whole organ analysis. This led us to evaluate the lignin deposition in situ, at the maturation zone, where cells no longer elongate (Figure 1b). It is in this root segment where lignin deposition is triggered as a defence reaction when a root pathogen approximates or pre-penetrates a root (Mandal and Mitra, 2007). In this study, taking advantage of the auto-fluorescent properties of cell wall biopolymers, confocal microscopy was used to estimate lignin and suberin content after *F. virguliforme* inoculation in local and systemic root tissues. Lignin deposition occurred mainly at the epidermis in the local tissues (FvA). In addition, hypodermis and cortex showed a higher lignin deposition in the inoculated roots compared to the non-inoculated ones, regardless of the distance to the inoculation point (FvA and FvD; Figure 3b). Interestingly, plants deposited lignin systemically in response to the fungus. Histochemical studies in *Brassica napus* revealed that the phenolics compounds and lignin deposition seems to be involved in vascular obstruction and reinforcement of tracheary elements during the early defence against Verticillium longisporum (Eynck et al. 2009). Particularly in the case of SDS, cell wall strengthness by

lignin deposition is very important since *F. virguliforme* hydrolytic enzymes may play a major role in root necrosis during late infection stages (Sahu et al. 2017). A significant lignin deposition increase was detected in inoculated plants (FvA and FvD) at 48 and 96 hpi (Figure 3a). Curiously, although a gradual lignin deposition increase over time was expected, results showed a return to basal levels (not significant differences) at 72 hpi. This oscillation may be a consequence of the high variability in maturation stages of the experimental units (the segments of the maturation zone) which must be destructively sampled for the microscopic observation. An in-vivo following up of lignin deposition along time in each individual root, would have avoided this artifact.

In this work, suberin was detected in every evaluated condition. Suberin is constitutively deposited in root endodermal and peridermal cell walls (Vishwanath et. al, 2015). However, a high suberization level in the local tissues (FvA), in both the epidermis and the hypodermis cells, was evidenced. Confocal microscopy results showed that after fungus inoculation, suberin was first deposited, followed by lignin. Interestingly, this increment in suberitation was detected before the pathogen reached the root surface (i.e. 24 hpi), while lignification started 48 hours later, when *F. virguliforme* contacted the root surface. Genome sequencing of *F. virguliforme* identified putative pathogenicity genes. Among them there were genes that may be associated with cell wall degradation in root tissues (Srivastava et al 2014). Results presented in this study, suggest that the plant is capable of detecting the pathogen secreted molecules during the early infection stage and inducing suberin deposition near the *F. virguliforme* entrance to delay fungus infection in the roots. There are several reports of pathogen eliciting suberin deposition in the host cell walls within and around the infection site, limiting the spread (Kolattukudy and Espelie, 1989). Thomas et al. (2007) demonstrated that preformed suberin reduced soybean susceptibility to Phytophthora sojae, suggesting a

relationship between suberin deposition and disease resistance. The suberization might be an interesting target to improve plant resistance against pathogens. In addition, suberin associated compounds (i.e. wax or phenolics components) may have antifungal properties (Lulai and Corsini 1998).

A considerable number of genes encoding cell wall and plasma membrane proteins were induced in soybean roots after *F. virguliforme* infection (Ngaki et al. 2016). Particularly, the phenylpropanoid pathway genes are highly expressed in biotic stress conditions (Yadav et. at. 2020). In this work we evaluated the expression dynamics of three of those genes: PAL, HCT and CAD. As result, the expression induction by *F. virguliforme* of the three evaluated genes was observed even before the root-hyphae contact (24 hpi) and correlated with the cell wall modifications in the adjacent area (FvA). Marquez et al. (2019) demonstrated that the phenylpropanoid biosynthesis pathway showed the highest number of differentially expressed genes upon *F. virguliforme* infection. Phenylpropanoid metabolism pathway generates lignin precursors, flavonoids and other aromatic metabolites like coumarins, volatile phenolic compounds, or tannins (Cheynier et al. 2013). This suggests that the premature activation of the phenylpropanoid biosynthesis pathway may result in the plant cell resistance to the pathogen entry through incrementing a wide variety of precursors, as structural and/or signalling molecules. A similar response was observed in resistant ginger against Pythium, a necrotrophic soil-borne that causes soft-rot disease (Geetha et al. 2019).

In conclusion, results presented in this work provide further evidence of an induced increment of lignin and suberin deposition specifically in the infection site of *F. virguliforme* in soybean roots. This event is probably part of the plant defence response intended to avoid the pathogen income or at least to delay pathogen invasion, giving the host more time to prepare the defence strategy. Strikingly, these results suggest that the roots not only trigger

371 cell wall strengthening near the pathogen entry, but also in distant areas where strengthening
372 of hypodermis and cortex was observed.
373
374 **ACKNOWLEDGEMENTS**
375 This study was supported by the INTA's research funds (PNPV-1135024). The authors would
376 like to thank Dr. Gaston Vaghi Medina for his helpful suggestions and critical reading of the
377 manuscript.
378
379 **AUTHOR CONTRIBUTIONS**
380 MLG, NM, LO and DAD conceived and planned the experiments. MLG carried out the
381 experiment, took and prepared the samples for confocal microscope observation, analysed
382 the data and took the lead in writing the manuscript. NM and LO contributed to the analysis
383 of the results and to the writing of the manuscript. LO contributed to sample preparation and
384 confocal microscopy observations.
385 All authors provided critical feedback and helped shape the research, analysis and
386 manuscript.
387
388 **REFERENCES**
389 Abeysekara NS, Bhattacharyya MK (2014). Analyses of the Xylem Sap Proteomes Identified
390 Candidate *Fusarium virguliforme* Proteinacious Toxins. PLOS ONE, 9(5), e93667.
391 https://doi.org/10.1371/journal.pone.0093667
392 Aoki T, O'Donnell K, Scandiani MM (2005). Sudden death syndrome of soybean in South
393 America is caused by four species of Fusarium: Fusarium brasiliense sp. nov., F.

394 cuneirostrum sp. nov., F. tucumaniae, and *F. virguliforme*. Mycoscience, 46(3), 162–183.
395 doi:10.1007/s10267-005-0235-y
396 Aoki T, Scandiani MM, O'Donnell, K (2012). Phenotypic, molecular phylogenetic, and
397 pathogenetic characterization of Fusarium crassistipitatum sp. nov., a novel soybean sudden
398 death syndrome pathogen from Argentina and Brazil. Mycoscience, 53(3), 167–186.
399 doi:10.1007/s10267-011-0150-3
400 Barros J, Serk H, Granlund I, Pesquet E (2015). The cell biology of lignification in higher
401 plants. Annals of Botany, 115(7), 1053–1074. doi:10.1093/aob/mcv046
402 Bonello P, Storer AJ, Gordon TR, Wood DL, Heller W (2003). Systemic Effects of
403 Heterobasidion annosum on Ferulic Acid Glucoside and Lignin of Presymptomatic
404 Ponderosa Pine Phloem, and Potential Effects on Bark-Beetle-Associated Fungi. Journal of
405 Chemical Ecology, 29(5), 1167–1182. doi:10.1023/A:1023833707382
406 Brar HK, Swaminathan S, Bhattacharyya MK (2011). The *Fusarium virguliforme* Toxin
407 FvTox1 Causes Foliar Sudden Death Syndrome-Like Symptoms in Soybean. Molecular
408 Plant-Microbe Interactions®, 24(10), 1179–1188. doi:10.1094/MPMI-12-10-0285
409 Buendgen MR, Coors JG, Grombacher AW, Russell WA (1990). European Corn Borer
410 Resistance and Cell Wall Composition of Three Maize Populations (Scriber and Slansky ,
411 1981). Elevated levels of indigestible fiber and silica may increase the bulk density of the
412 diet to the point that insects are unable to ingest, 510, 505–510.
413 Chang HX, Yendrek CR, Caetano-Anolles G, Hartman GL (2016). Genomic characterization
414 of plant cell wall degrading enzymes and in silico analysis of xylanses and
415 polygalacturonases of *Fusarium virguliforme*. BMC Microbiology, 16(1), 1–12.
416 doi:10.1186/s12866-016-0761-0

417 Cheynier V, Comte G, Davies KM, Lattanzio V, Martens S (2013). Plant phenolics: recent
418 advances on their biosynthesis, genetics, and ecophysiology. Plant physiology and
419 biochemistry, 72, 1-20.
420 Declerck S, Strullu DG, Plenchette C (1998). Monoxenic culture of the intraradical forms of
421 Glomus sp. isolated from a tropical ecosystem: a proposed methodology for germplasm
422 collection. Mycologia, 90(4), 579–585. doi:10.1080/00275514.1998.12026946
423 Di Rienzo JA, Casanoves F, Balzarini MG, Gonzalez L, Tablada M, Robledo CW (2008).
424 InfoStat, versión 2008. Grupo InfoStat, FCA, Universidad Nacional de Córdoba, Argentina.
425 Engelsdorf T, Gigli-Bisceglia N, Veerabagu M, McKenna JF, Vaahtera L, Augstein F, et al.
426 (2018). The plant cell wall integrity maintenance and immune signaling systems cooperate
427 to control stress responses in Arabidopsis thaliana; Science Signaling, 11(536)
428 doi:10.1126/scisignal.aao3070
429 Eynck C, Koopmann B, Karlovsky P, von Tiedemann A (2009). Internal Resistance in Winter
430 Oilseed Rape Inhibits Systemic Spread of the Vascular Pathogen Verticillium longisporum.
431 Phytopathology, 99(7), 802–811. doi:10.1094/PHYTO-99-7-0802
432 FAOstat (2021). Food and Agriculture Organization of the United Nations.
433 [http://www.fao.org/faostat/en/#data/QC/visualize]. Accessed 03 March 2022.
434 Ferrari S, Savatin D, Sicilia F, Gramegna G, Cervone F, De Lorenzo G (2013).
435 Oligogalacturonides: plant damage-associated molecular patterns and regulators of growth
436 and development. Frontiers in Plant Science.
437 https://www.frontiersin.org/article/10.3389/fpls.2013.00049
438 Franke R, Schreiber L (2007). Suberin — a biopolyester forming apoplastic plant interfaces.
439 Current Opinion in Plant Biology, 10(3), 252–259.
440 doi:https://doi.org/10.1016/j.pbi.2007.04.004

441 Geetha KA, Koyyappurath S, Augustine L, Thomas G (2019). Transcriptional analysis and
442 histochemistry reveal a dominant role for cell wall signaling in mediating Pythium
443 myriotylum resistance in Zingiber zerumbet. Physiological and Molecular Plant Pathology,
444 106, 7–15. doi:10.1016/j.pmpp.2018.11.002
445 Giachero ML, Marquez N, Gallou A, Luna CM, Declerck S, Ducasse DA (2017). An in vitro
446 method for studying the three-way interaction between soybean, Rhizophagus irregularis and
447 the soil-borne pathogen *Fusarium virguliforme*. Frontiers in Plant Science, 8.
448 doi:10.3389/fpls.2017.01033
449 Gongora-Canul CC, Leandro LFS (2011). Effect of Soil Temperature and Plant Age at Time
450 of Inoculation on Progress of Root Rot and Foliar Symptoms of Soybean Sudden Death
451 Syndrome. Plant Disease, 95(4), 436–440. doi:10.1094/PDIS-07-10-0489
452 Hu R, Fan C, Li H, Zhang Q, Fu YF (2009). Evaluation of putative reference genes for gene
453 expression normalization in soybean by quantitative real-time RT-PCR. BMC Molecular
454 Biology, 10 (May 2014), 93. doi:10.1186/1471-2199-10-93
455 Hutzler P, Fischbach R, Heller W, Jungblut TP, Reuber S, Schmitz R, et al. (1998). Tissue
456 localization of phenolic compounds in plants by confocal laser scanning microscopy. Journal
457 of Experimental Botany, 49(323), 953–965. doi:10.1093/jxb/49.323.953
458 Iqbal MJ, Yaegashi S, Ahsan R, Shopinski KL, Lightfoot DA (2005). Root response to
459 Fusarium solani f. sp. glycines: Temporal accumulation of transcripts in partially resistant
460 and susceptible soybean. Theoretical and Applied Genetics, 110(8), 1429–1438.
461 doi:10.1007/s00122-005-1969-9
462 Islam KT, Bond JP, Fakhoury AM (2017). FvSNF1, the sucrose non-fermenting protein
463 kinase gene of *Fusarium virguliforme*, is required for cell-wall-degrading enzymes

464 expression and sudden death syndrome development in soybean. Current Genetics, 63(4),
465 723–738. doi:10.1007/s00294-017-0676-9
466 Kolattukudy PE (2001). Polyesters in Higher Plants BT - Biopolyesters. In W. Babel & A.
467 Steinbüchel (Eds.), (pp. 1–49). Berlin, Heidelberg: Springer Berlin Heidelberg.
468 doi:10.1007/3-540-40021-4_1
469 Kolattukudy PE, Espelie KE (1989). Chemistry, Biochemistry, and Function of Suberin and
470 Associated Waxes BT - Natural Products of Woody Plants: Chemicals Extraneous to the
471 Lignocellulosic Cell Wall. In J. W. Rowe (Ed.), (pp. 304–367). Berlin, Heidelberg: Springer
472 Berlin Heidelberg. doi:10.1007/978-3-642-74075-6_11
473 Liu CJ, Miao YC, Zhang KW (2011). Sequestration and Transport of Lignin Monomeric
474 Precursors. Molecules, 16(1), 710–727. doi:10.3390/molecules16010710
475 Liu Q, Luo L, Zheng L (2018). Lignins: Biosynthesis and biological functions in plants.
476 International Journal of Molecular Sciences, 19(2). doi:10.3390/ijms19020335
477 Livak KJ, Schmittgen TD (2001). Analysis of Relative Gene Expression Data Using Real-
478 Time Quantitative PCR and the 2−ΔΔCT Method. Methods, 25(4), 402–408.
479 doi:10.1006/meth.2001.1262
480 Lozovaya VV, Lygin a V, Zernova OV, Li S, Widholm JM, Hartman GL (2006). Lignin
481 degradation by Fusarium solani f. sp glycines. Plant Disease, 90(1), 77–82. doi:Doi
482 10.1094/Pd-90-0077
483 Lozovaya VV, Lygin AV, Zernova OV, Li S, Hartman GL, Widholm JM (2004).
484 Isoflavonoid accumulation in soybean hairy roots upon treatment with Fusarium solani. Plant
485 Physiology and Biochemistry, 42(7–8), 671–679. doi:10.1016/j.plaphy.2004.06.007
486 Lulai EC, Corsini DL (1998). Differential deposition of suberin phenolic and aliphatic
487 domains and their roles in resistance to infection during potato tuber (Solanum tuberosum

488 L.) wound-healing. Physiological and Molecular Plant Pathology, 53(4), 209–222.
489 doi:https://doi.org/10.1006/pmpp.1998.0179

490 Mandal S, Mitra A (2007). Reinforcement of cell wall in roots of Lycopersicon esculentum
491 through induction of phenolic compounds and lignin by elicitors. Physiological and
492 Molecular Plant Pathology, 71(4–6), 201–209. doi:10.1016/j.pmpp.2008.02.003

493 Marquez N, Giachero ML, Gallou A, Debat HJ, Declerck S, Ducasse DA (2019).
494 Transcriptome analysis of mycorrhizal and nonmycorrhizal soybean plantlets upon infection
495 with *Fusarium virguliforme*, one causal agent of sudden death syndrome. Plant Pathology,
496 68(3), 470–480. doi:10.1111/ppa.12964

497 Menden B, Kohlhoff M, Moerschbacher BM (2007). Wheat cells accumulate a syringyl-rich
498 lignin during the hypersensitive resistance response. Phytochemistry, 68(4), 513–520.
499 doi:10.1016/j.phytochem.2006.11.011

500 Misas-Villamil JC, van der Hoorn RAL (2008). Enzyme-inhibitor interactions at the plant-
501 pathogen interface. Current Opinion in Plant Biology, 11(4), 380–388.
502 doi:10.1016/j.pbi.2008.04.007

503 Moreira-Vilar FC, Siqueira-Soares RDC, Finger-Teixeira A, Oliveira DMD, Ferro AP, da
504 Rocha GJ, et al. (2014). The acetyl bromide method is faster, simpler and presents best
505 recovery of lignin in different herbaceous tissues than klason and thioglycolic acid methods.
506 PLoS ONE, 9(10), e110000. doi:10.1371/journal.pone.0110000

507 Moura JCMS, Bonine CAV, de Oliveira Fernandes Viana J, Dornelas MC, Mazzafera P
508 (2010). Abiotic and biotic stresses and changes in the lignin content and composition in
509 plants. Journal of Integrative Plant Biology, 52(4), 360–376. doi:10.1111/j.1744-
510 7909.2010.00892.x

511 Ngaki MN, Wang B, Sahu BB, Srivastava SK, Farooqi MS, Kambakam S, ... and
512 Bhattacharyya MK (2016). Transcriptomic study of the soybean-*Fusarium virguliforme*
513 interaction revealed a novel ankyrin-repeat containing defense gene, expression of whose
514 during infection led to enhanced resistance to the fungal pathogen in transgenic soybean
515 plants. PloS one, 11(10), e0163106.

516 Navi SS, Yang XB (2008). Foliar symptom expression in association with early infection and
517 xylem colonization by *Fusarium virguliforme* (formerly F. solani f. sp. glycines), the causal
518 agent of soybean Sudden Death Syndrome. Plant Health Progress, 9(1), 24. doi:10.1094/php-
519 2008-0222-01-rs

520 Radwan O, Liu Y, Clough SJ (2011). Transcriptional analysis of soybean root response to
521 *Fusarium virguliforme*, the causal agent of Sudden Death Syndrome. Molecular Plant-
522 Microbe Interactions, 24(8), 958–972. doi:10.1094/MPMI-11-10-0271

523 Roy KW (1997). Fusarium solani on soybean roots: nomenclature of the causal agent of
524 Sudden Death Syndrome and identity and relevance of F. solani form B. Plant Disease, 81(3),
525 259–266. doi:10.1094/PDIS.1997.81.3.259

526 Roy KW, State M, Rupe JC, Hershman DE, Abney TS, Lafayette W, et al. (1997). Sudden
527 Death Syndrome of soybean. Plant Disease, 81(10), 1100–1111.
528 doi:https://doi.org/10.1094/PDIS.1997.81.10.1100

529 Rupe JC, Correll JC, Guerber JC, Becton CM, Gbur Jr EE, Cummings MS, Yount PA (2001).
530 Differentiation of the Sudden Death Syndrome pathogen of soybean, Fusarium solani f. sp.
531 glycines, from other isolates of F. solani based on cultural morphology, pathogenicity, and
532 mitochondrial DNA restriction fragment length polymorphism. Canadian Journal of Botany,
533 79(7), 829–835. doi:10.1139/cjb-79-7-829

534 Sahu BB, Baumbach JL, Singh P, Srivastava SK, Yi X, Bhattacharyya MK (2017).
535 Investigation of the *Fusarium virguliforme* transcriptomes induced during infection of
536 soybean roots suggests that enzymes with hydrolytic activities could play a major role in root
537 necrosis. PLoS ONE, 12(1), 1–22. doi:10.1371/journal.pone.0169963
538 Schindelin J, Arganda-Carreras I, Frise E, Kaynig V, Longair M, Pietzsch T, et al. (2012).
539 Fiji: an open-source platform for biological-image analysis. Nature Methods, 9(7), 676–682.
540 doi:10.1038/nmeth.2019
541 Smit F, Dubery IA (1997). Cell wall reinforcement in cotton hypocotyls in response to a
542 Verticillium dahliae elicitor. Phytochemistry, 44(5), 811–815. doi:10.1016/S0031-
543 9422(96)00595-X
544 Souza C de A, Li S, Lin AZ, Boutrot F, Grossmann G, Zipfel C, Somerville SC (2017).
545 Cellulose-derived oligomers act as damage-associated molecular patterns and trigger
546 defense-like responses. Plant Physiology, 173(4), 2383–2398. doi:10.1104/pp.16.01680
547 Spampinato CP, Scandiani MM, Luque AG (2021). Soybean Sudden Death Syndrome:
548 Fungal pathogenesis and plant response. Plant Pathology, 70(1), 3–12.
549 doi:10.1111/ppa.13275
550 Srivastava SK, Huang X, Brar HK, Fakhoury AM, Bluhm BH, Bhattacharyya MK (2014).
551 The genome sequence of the fungal pathogen *Fusarium virguliforme* that causes Sudden
552 Death Syndrome in soybean. PLoS ONE, 9(1). doi:10.1371/journal.pone.0081832
553 Thomas R, Fang X, Ranathunge K, Anderson TR, Peterson CA, Bernards MA (2007).
554 Soybean root suberin: anatomical distribution, chemical composition, and relationship to
555 partial resistance to Phytophthora sojae. Plant Physiology, 144(1), 299–311.
556 doi:10.1104/pp.106.091090

557 Tippett JT, Hill TC (1984). Role of periderm in resistance of Eucalyptus marginata roots
558 against Phytophthora cinnamomi. European Journal of Forest Pathology, 14(7), 431–439.
559 doi:https://doi.org/10.1111/j.1439-0329.1984.tb01256.x
560 Vaughn SF, Lulai EC (1991). The involvement of mechanical barriers in the resistance
561 response of a field-resistant and a field-susceptible potato cultivar to Verticillium dahliae.
562 Physiological and Molecular Plant Pathology, 38(6), 455–465.
563 doi:https://doi.org/10.1016/S0885-5765(05)80113-4
564 Vishwanath SJ, Delude C, Domergue F, Rowland O (2015). Suberin: biosynthesis,
565 regulation, and polymer assembly of a protective extracellular barrier. Plant Cell Reports,
566 34(4), 573–586. doi:10.1007/s00299-014-1727-z
567 Wang S (2020). Recent insights into plant-pathogens interactions through proteomics
568 approaches. IOP Conference Series: Materials Science and Engineering, 768, 52050.
569 doi:10.1088/1757-899x/768/5/052050
570 Wolf S (2017). Plant cell wall signalling and receptor-like kinases. Biochemical Journal,
571 474(4), 471–492. doi:10.1042/BCJ20160238
572 Wrather A, Shannon G, Balardin R, Carregal L, Escobar R, Gupta GK, et al. (2010). Effect
573 of diseases on soybean yield in the top eight producing countries in 2006. Plant Health
574 Progress, 11(1), 29. doi:10.1094/php-2010-0102-01-rs
575 Wuyts N, Lognay G, Swennen R, De Waele D (2006). Nematode infection and reproduction
576 in transgenic and mutant Arabidopsis and tobacco with an altered phenylpropanoid
577 metabolism. Journal of Experimental Botany, 57(11), 2825–2835. doi:10.1093/jxb/erl044
578 Yadav V, Wang Z, Wei C, Amo A, Ahmed B, Yang X, Zhang X (2020). Phenylpropanoid
579 pathway engineering: An emerging approach towards plant defense. Pathogens, 9(4), 1–25.
580 doi:10.3390/pathogens9040312

581 Zhong R, Lee C, McCarthy RL, Reeves CK, Jones EG, Ye ZH (2011). Transcriptional
582 activation of secondary wall biosynthesis by rice and maize NAC and MYB transcription
583 factors. Plant and Cell Physiology, 52(10), 1856–1871. doi:10.1093/pcp/pcr123

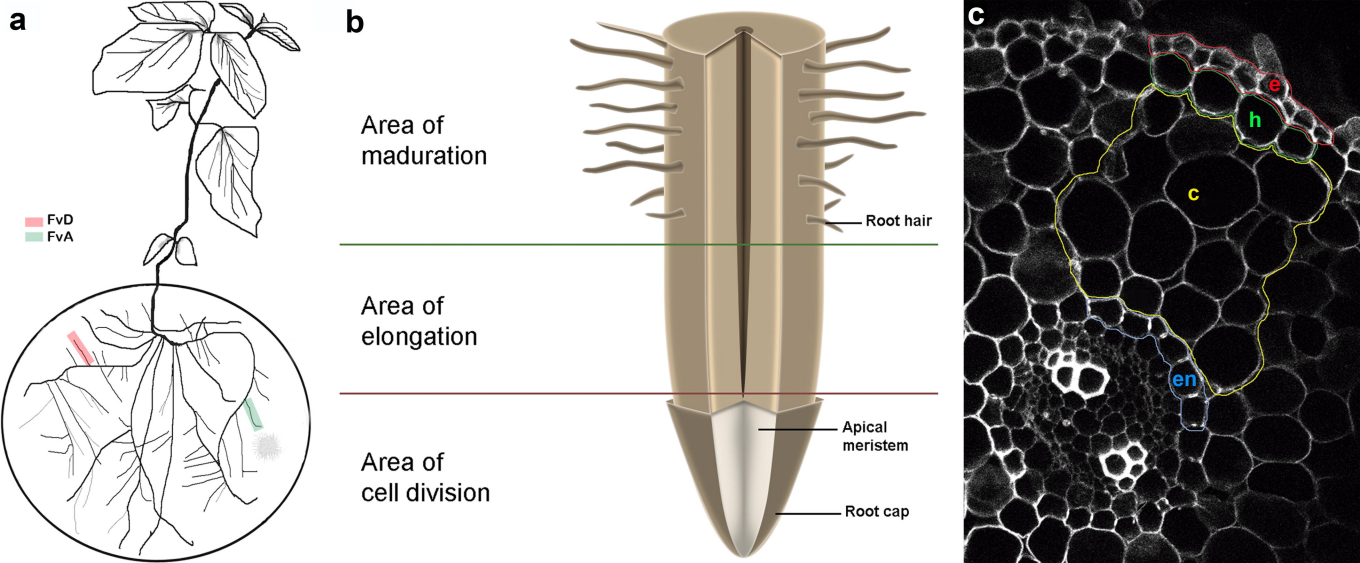
a
FvD
FvA
b
Area of maduration
Root hair
Area of elongation
Apical meristem
Area of cell division
Root cap
c
e
h
c
en

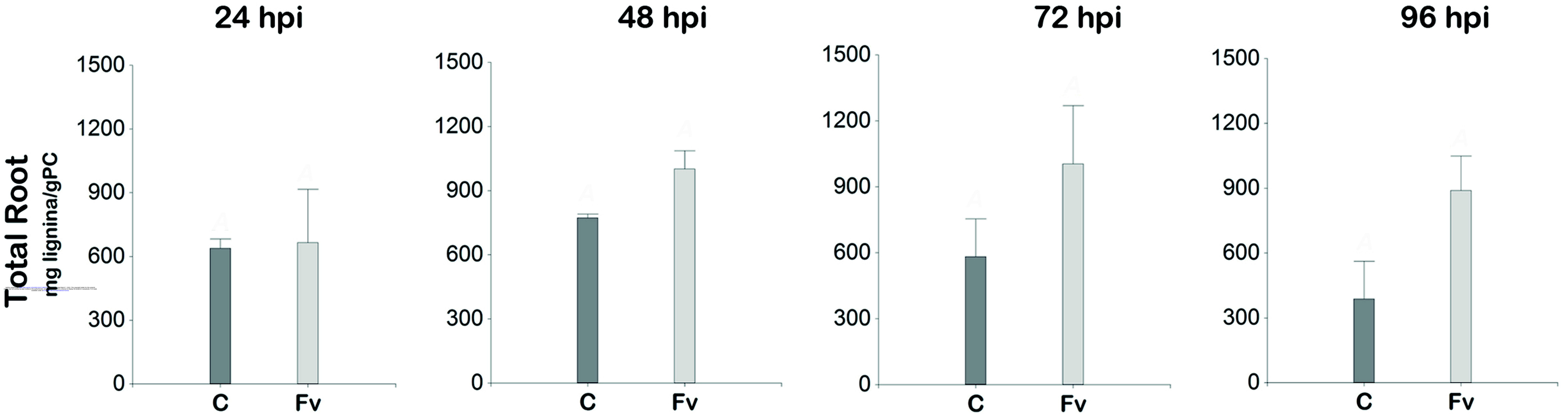
24 hpi
48 hpi
72 hpi
96 hpi
Total Root
mg lignina/gPC
1500
1200
900
600
300
0
C
Fv
A

Lignin

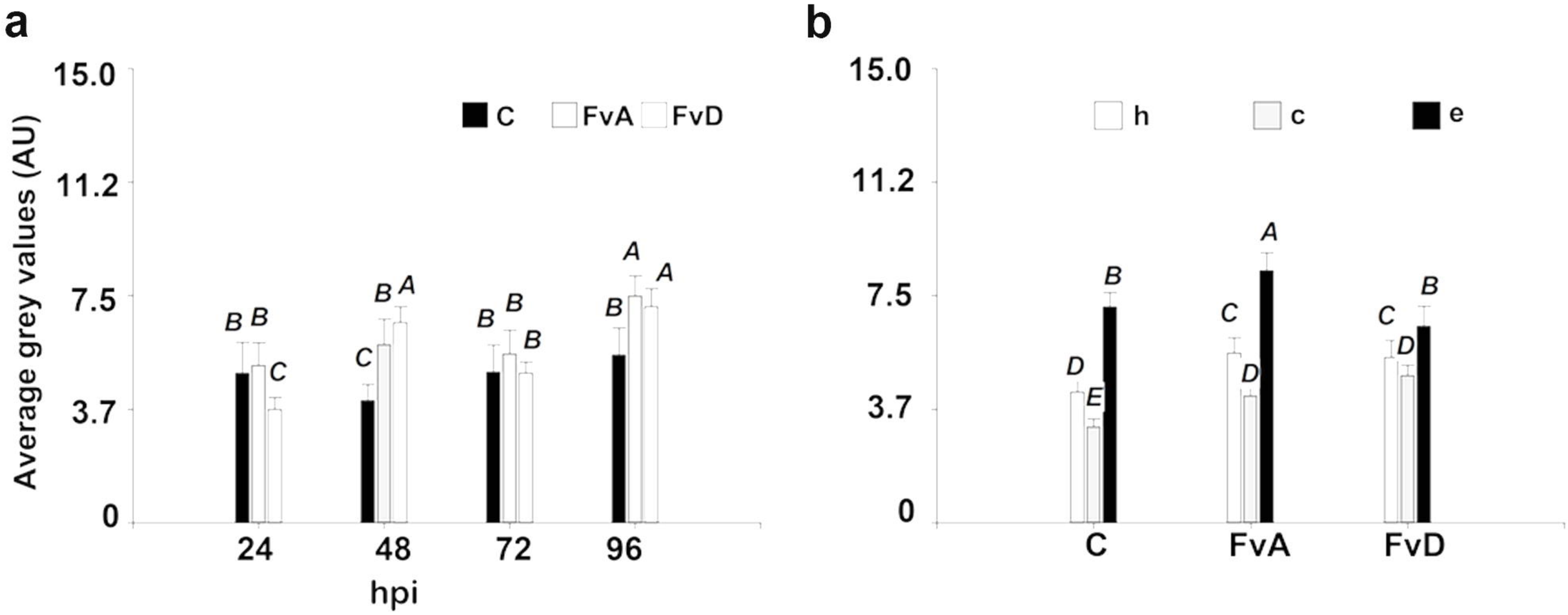

Suberin

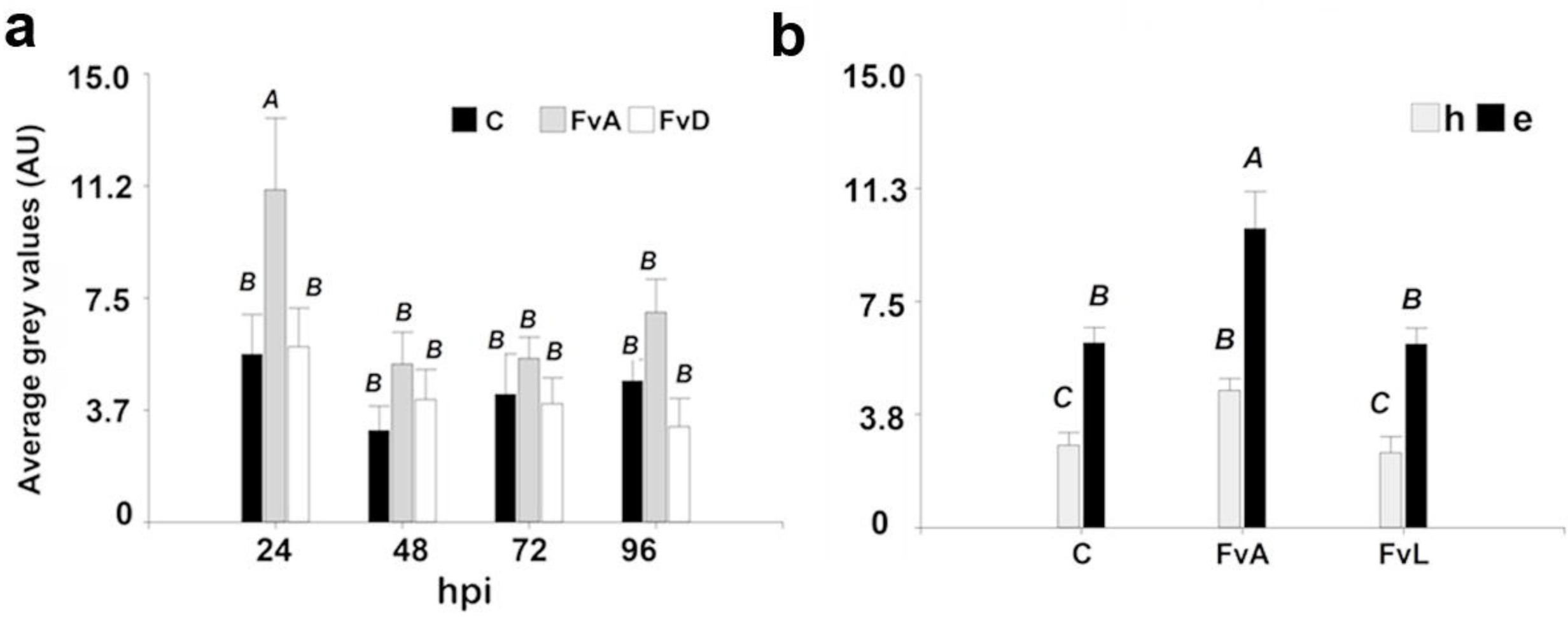

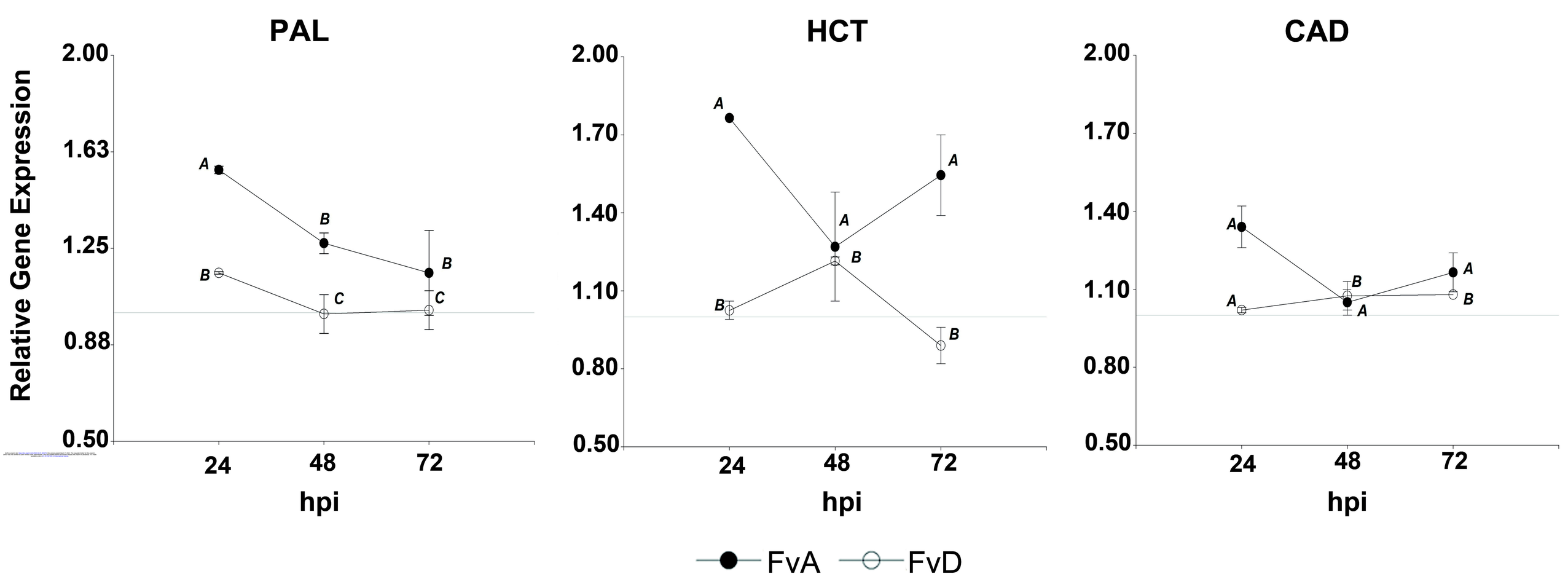
PAL
HCT
CAD
Relative Gene Expression
2.00
1.63
1.25
0.88
0.50
1.70
1.40
1.10
0.80
24
48
72
hpi
A
B
C
FvA
FvD